

GRANT AGREEMENT No.: 764902		 TOMOCON Smart Tomographic Sensors for Advanced Industrial Process Control	
Project Acronym: TOMOCON			
Project title: Smart tomographic sensors for advanced industrial process control			
Deliverable Rel. No. D2.2.	Lead Beneficiary UEF		
EU Del. No. D6	Type Report		
WP No. WP2	Date: 06.09.2019	Revision: 0	
Innovative Training Network TOMOCON			
Deliverable Title			
Virtual Process Tomography Data for TOMOCON Demonstrations			
Description			
<p>This deliverable describes the output data from the virtual tomographic sensors for the four industrial demonstration cases, including physical meaning, uncertainties, data formats, protocols and sampling frequencies.</p>			

Prepared by:	Prof. Dr. Marko Vauhkonen	
Approved by:	Prof. Dr. Uwe Hampel	
Approved by Supervisory Board:	17.09.2019	

Dissemination Level: **Public**



This project has received funding from the European Union's Horizon 2020 research and innovation programme under the Marie Skłodowska-Curie Grant Agreement No. 764902.

TOMOCON			GRANT AGREEMENT No.: 764902		
Deliverable Title: Virtual Process Tomography Data for TOMOCON Demonstrations					
Del. Rel. No.	EU Del. No.	WP No.	Lead Beneficiary	Type	Date
D2.2.	D6	WP2	UEF	Report	06.09.2019

Revision Sheet

Revision Number	Purpose of Revision	Effective Date
0	Initial Issue	17.09.2019



TOMOCON			GRANT AGREEMENT No.: 764902		
Deliverable Title: Virtual Process Tomography Data for TOMOCON Demonstrations					
Del. Rel. No.	EU Del. No.	WP No.	Lead Beneficiary	Type	Date
D2.2.	D6	WP2	UEF	Report	06.09.2019

Table of Contents

1. Tomographic sensors for virtual demonstration of inline fluid separation.....	4
1.1. Virtual wire-mesh sensor	4
1.2. Virtual ERT sensor	5
2. Tomographic sensors for the virtual demonstration of continuous casting	8
2.1. Virtual CIFT sensor	9
2.2. Virtual ECT/MIT sensor	9
3. Tomographic sensors for virtual demonstration of microwave drying	10
3.1. ECT.....	10
3.2. Microwave tomography	12
3.3. Visual analytics and interactive visualisation for process tomography virtual demonstration.....	16
4. Tomographic sensors for virtual demonstration of semi-batch crystallization	18
4.1. Impedance tomography in semi-batch crystallization.....	18
4.2. Ultrasound computed tomography for semi-batch crystallization	19
4.3. Tomographic output data in PID controller design of a crystallization process	20



TOMOCON			GRANT AGREEMENT No.: 764902		
Deliverable Title: Virtual Process Tomography Data for TOMOCON Demonstrations					
Del. Rel. No.	EU Del. No.	WP No.	Lead Beneficiary	Type	Date
D2.2.	D6	WP2	UEF	Report	06.09.2019

1. Tomographic sensors for virtual demonstration of inline fluid separation

Gas-liquid separation using a swirl element mounted inside a pipe instead of gravity-driven separators is an approach for the multiphase flow being used in process industries. The vortex created by the swirl element varies in shape and size. To improve the split efficiency, the size of the vortex should be known in such a manner that it does not disturb the flow. In this demonstration, Electrical Tomography will be used as a non-intrusive visualization method to estimate the size of the vortex. Additionally the wire-mesh sensor will measure upstream conditions and send this information to the controller. This information can be used to take corrective actions before an unwanted flow/disturbance (like a plug) reaches the swirl element. Thus, the effect of the disturbance will be reduced by measuring it and generating a control signal that counteracts it.

1.1. Virtual wire-mesh sensor

Wire-mesh sensors consist of two planes of parallel wires placed in a pipe cross-section. The wires are separated by a short distance and arranged in a way that they form an angle of 90° to each other. In the one plane (transmitter), wires are sequentially activated with a voltage while at the (receiver) wires in the other plane transmitted electrical currents are simultaneously measured (Figure 1, left). This way the electrical properties in the crossing-points are obtained with a high-speed rate of 10,000 frames per second. It should be noted that two types of wire-mesh sensors exist which work on measuring electrical properties of fluids. The conductivity type will be used for air/water measurement (Figure 1, right), where the local instantaneous conductance is direct proportional to the amount of water within the single crossing point.

A wire-mesh sensor is placed upstream of the swirl element as shown in Figure 2. It is ideal for measuring flow characteristics of the incoming air/water mixture. Information from both sensors, WMS and ECT, will be forwarded to a control unit for further data processing.

A virtual sensor will be programmed in MATLAB®/SIMULINK® to imitate a real sensor. The data from the virtual sensor will be collected in form of frames. These frames will come from measurement data collected by a real wire-mesh sensor, which are obtained from experiments done at the TOPLOW+ facility in HZDR. The virtual sensor will sample each second frame from the initial data giving the virtual sensor a rate of 5000 frames per second compared to a real wire-mesh sensor. The virtual sensor data will be in 3D-matrix form. The output of the sensor will represent characteristic variables (e.g. cross-sectional averaged void fraction), which are used to describe the mathematical state of the dynamic system. These variables will continuously supply the controller with information at a frequency of 1 kHz. Research done at HZDR has proven that the sensor is able to predict the average core diameter within a certainty of ±10%. This information will be sent to our colleagues at Lodz University of Technology to simulate the gas core downstream.



TOMOCON			GRANT AGREEMENT No.: 764902		
Deliverable Title: Virtual Process Tomography Data for TOMOCON Demonstrations					
Del. Rel. No.	EU Del. No.	WP No.	Lead Beneficiary	Type	Date
D2.2.	D6	WP2	UEF	Report	06.09.2019

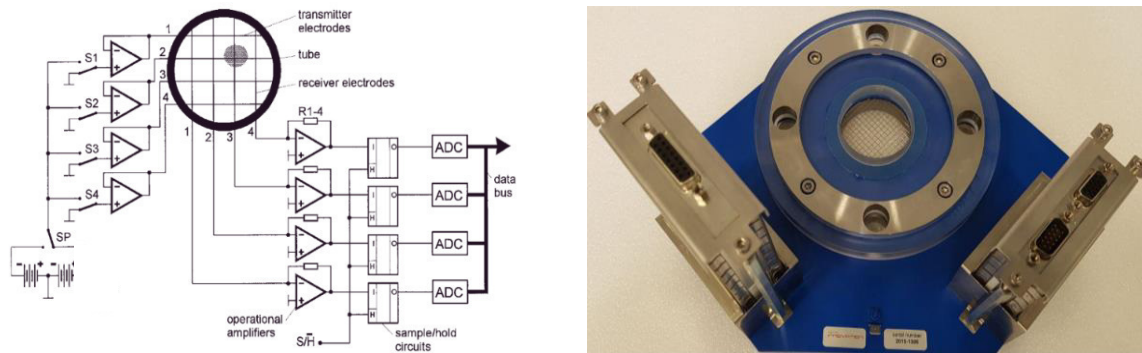


Figure 1: Schematics of a conductivity wire-mesh sensor (left), conductivity wire-mesh sensor (right)

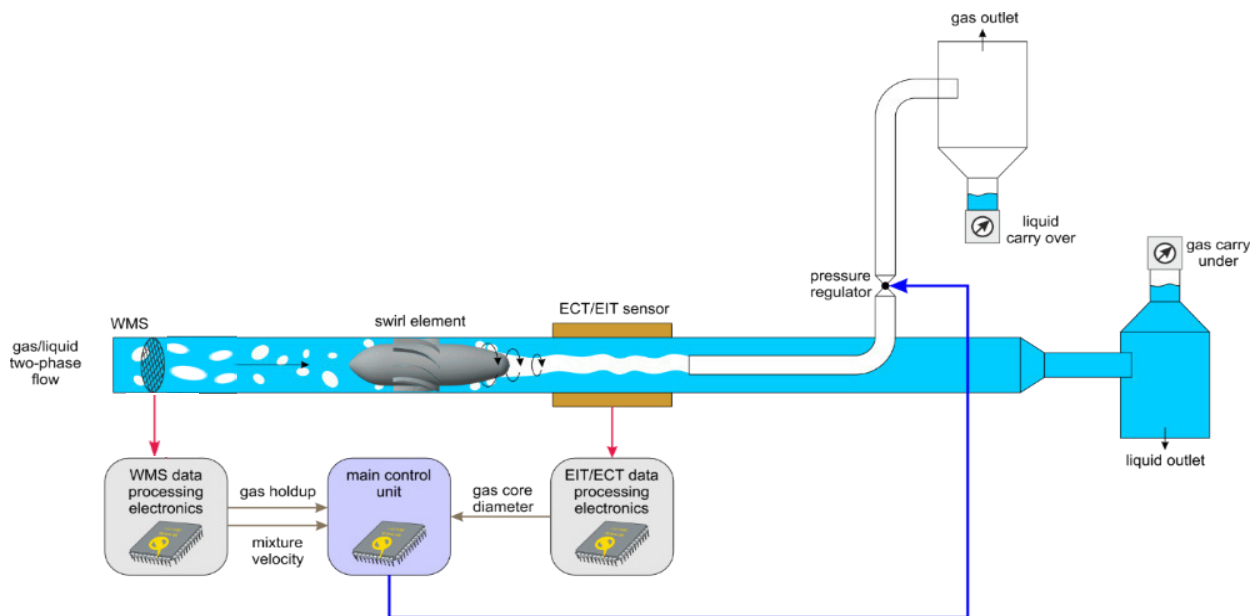


Figure 2: Dynamic system with tomography-controlled inline fluid separation for water-air separation

1.2. Virtual ERT sensor

A single layer of 16 stainless steel electrodes with a side length of 12mm which were evenly distributed on the inner surface of a 90 mm diameter PVC pipe is shown in Fig. 3. The distance between each electrode is 2.7 mm and attached to electronics using signal-conditioning units. Different flow regimes are currently being tested using 2D/2.5D image reconstructions and raw data analysis.



TOMOCON			GRANT AGREEMENT No.: 764902		
Deliverable Title: Virtual Process Tomography Data for TOMOCON Demonstrations					
Del. Rel. No.	EU Del. No.	WP No.	Lead Beneficiary	Type	Date
D2.2.	D6	WP2	UEF	Report	06.09.2019

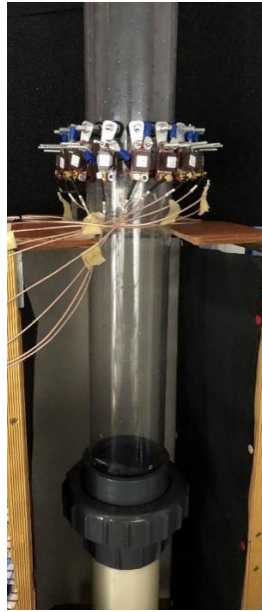


Figure 3: ET sensor for IFS

For the virtual demonstration the same sensor as real is replicated using EIDORS 3.9.1, a free software algorithm for forward and inverse modelling for Electrical Impedance Tomography.

Using EIDORS, 16 pin shaped electrodes are modelled and a mesh of 6048 elements is created both for forward and inverse problems, image reconstruction and analysis. To simulate the produced gas core we have used a set of data and an inhomogeneity factor. The set of data are the experimental measurements of the gas core diameter sent from HZDR. The inhomogeneity factor introduces different positions for the center of the gas core. This whole program will be converted to a SIMULINK block (as shown in Fig. 4) and will be integrated with the work of other partners. The output of this SIMULINK block is a single value that represents the radius of the vortex that is obtained using image processing techniques. This value will later be used to design a controller. The whole model is described in Fig. 5. In the virtual demonstration and also in the real measurement case, the temporal resolution of the ERT system is around 16 Hz, as far as data acquisition is concerned.



TOMOCON				GRANT AGREEMENT No.: 764902	
Deliverable Title: Virtual Process Tomography Data for TOMOCON Demonstrations					
Del. Rel. No.	EU Del. No.	WP No.	Lead Beneficiary	Type	Date
D2.2.	D6	WP2	UEF	Report	06.09.2019

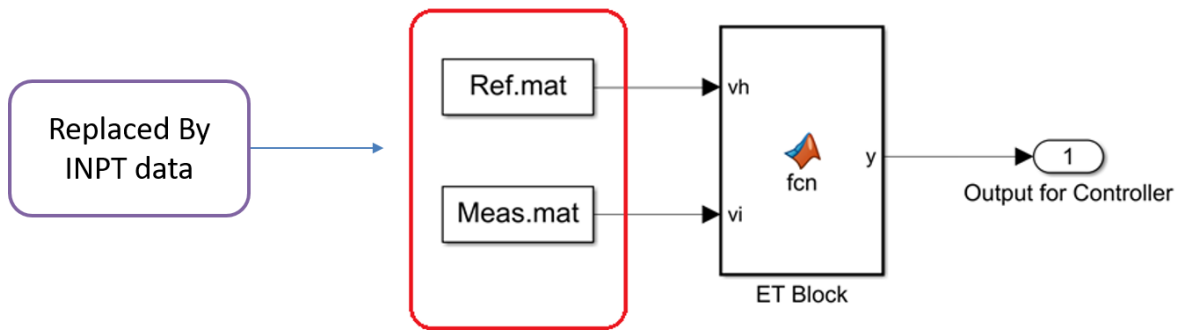


Figure 4: SIMULINK block for IFS VD

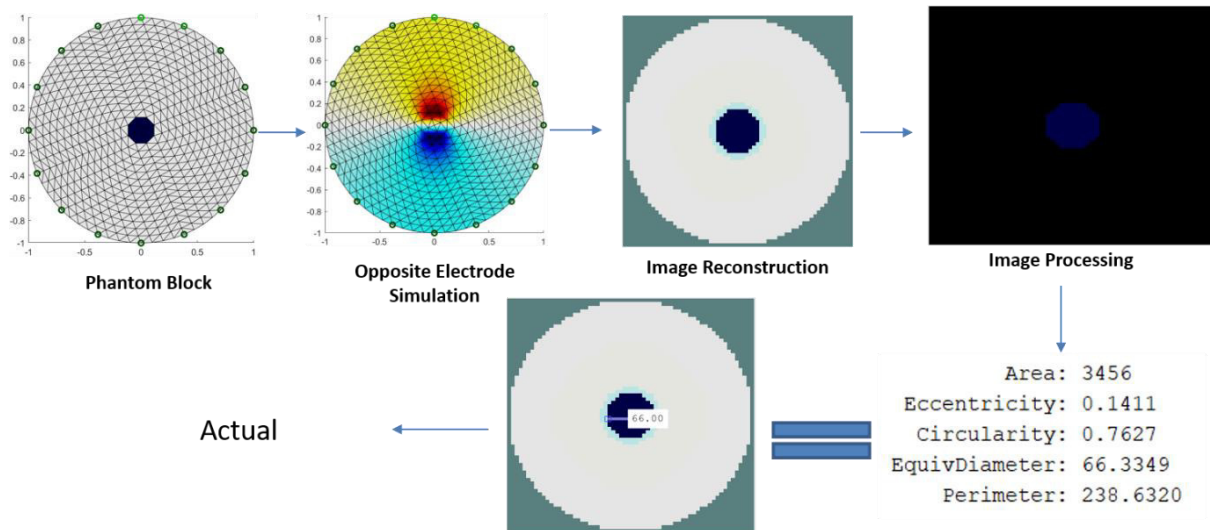


Figure 5: EIDORS model for virtual demonstration



TOMOCON				GRANT AGREEMENT No.: 764902	
Deliverable Title: Virtual Process Tomography Data for TOMOCON Demonstrations					
Del. Rel. No.	EU Del. No.	WP No.	Lead Beneficiary	Type	Date
D2.2.	D6	WP2	UEF	Report	06.09.2019

2. Tomographic sensors for the virtual demonstration of continuous casting

For continuous casting, three different sensor modalities will be used: Contactless Inductive Flow Tomography (CIFT) for the measurement of the two-dimensional flow field of the liquid metal in the mould and a combined sensor using Electrical Capacitance Tomography and Mutual Inductance Tomography (ECT/MIT) for visualizing the distribution of argon and liquid metal in the submerged entry nozzle (SEN). The CFD software OpenFOAM is utilized to calculate the transient behavior of the two-phase flow under the influence of the electromagnetic brake in the mould and the SEN. Therefore, all virtual sensors have been implemented in a file reader, which can directly access OpenFOAM cases. This data serves as an input to calculate the magnetic field for CIFT and MIT and the capacitance for ECT. In order to simulate the measurement uncertainty some defined noise will be added. This noisy raw data is then used for the reconstruction. The reconstructed images and the noisy raw data will be packed into a MATLAB or a JSON file. When the controller connects via TCP/IP to the virtual sensor, it can download the file. The controller then changes the according boundary conditions for the OpenFOAM simulation. This might be realized by selecting a different pre-computed OpenFOAM simulation, since the direct simulation of the flow according to the new boundary conditions is very time consuming and might need several days even on a large high performance computer. Figure 6 shows a schematic sketch of the data flow. In the following a detailed description of the virtual sensor for each modality will be given.

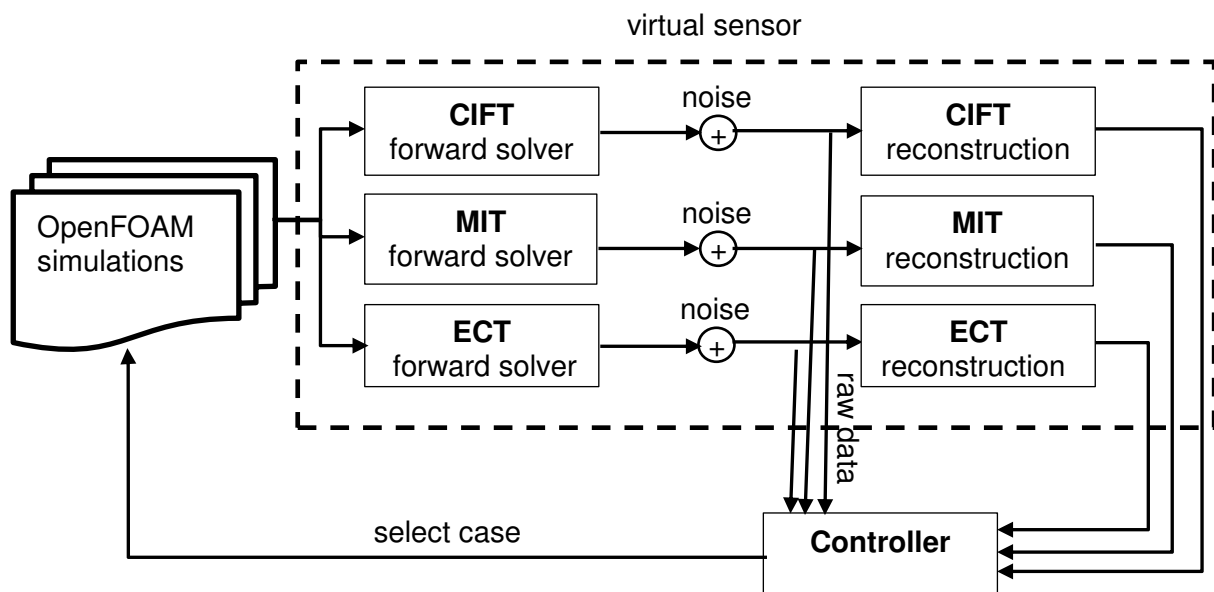


Figure 6: Schematic sketch of the virtual control loop and the virtual sensors

TOMOCON			GRANT AGREEMENT No.: 764902		
Deliverable Title: Virtual Process Tomography Data for TOMOCON Demonstrations					
Del. Rel. No.	EU Del. No.	WP No.	Lead Beneficiary	Type	Date
D2.2.	D6	WP2	UEF	Report	06.09.2019

2.1. Virtual CIFT sensor

The virtual CIFT sensor reads the velocity field in the mould from OpenFOAM and converts it to internal mesh for solving the forward problem. Then the flow induced magnetic field will be calculated at 7 virtual sensors along each narrow face of the mould for the applied magnetic field, which is generated by two excitation coils above and below the electromagnetic brake. The arrangement of the excitation coils as well as the 14 virtual sensors is in accordance with the planned physical realization of the sensor at the demonstrator. The calculated magnetic field is given in Tesla and a noise of about 5 nT will be added. The result will be used to calculate the reconstructed flow solving the inverse problem for CIFT. In a MATLAB or JSON file the noisy flow induced magnetic field and reconstructed flow structure in the mould in m/s on a coarse mesh will be transferred to the controller. The file contains the magnetic field for each sensor and the velocity field, which is stored as a list of coordinates with the velocity vector. Since the original velocity field will be available, the quality of the reconstruction can be calculated. It provides a TCP/IP server, where the controller can connect and download the data. The expected time resolution will be 1 Hz.

2.2. Virtual ECT/MIT sensor

The virtual ECT/MIT sensor reads at a given time interval the gas/liquid metal distribution in a defined volume of the SEN from OpenFOAM files and converts it to the internal mesh for solving the forward problem. Then, for MIT the induced voltages in the 8 detection coils will be calculated for a given excitation scheme, and in a similar way the capacitances for ECT with 8 electrodes will be calculated. After adding some noise to the result for each modality, the inverse problem will be solved. In a similar way as for CIFT, the noisy raw data and the reconstructed images will be presented via a TCP/IP server. The file contains the induce voltage or the capacitance at each sensor and the conductivity distribution, which is stored as a list of coordinates with the gas/liquid information as scalar field. The scalar field is a binary field, where 0 represents the liquid metal and 1 represents the gas. The expected time resolution will be about 100 Hz.



TOMOCON			GRANT AGREEMENT No.: 764902		
Deliverable Title: Virtual Process Tomography Data for TOMOCON Demonstrations					
Del. Rel. No.	EU Del. No.	WP No.	Lead Beneficiary	Type	Date
D2.2.	D6	WP2	UEF	Report	06.09.2019

3. Tomographic sensors for virtual demonstration of microwave drying

Drying of dielectric materials is one of the common processes in several industries. Among the main objectives of this process are adjusting non-uniform moisture distribution and reduction of energy consumption and processing time. Microwave heating technology makes the volumetric and selective heating possible. To benefit from its features, an advanced control system should be developed for distributed microwave sources. However, moisture distribution information and a process model are required to derive this controller. Fig. 7 shows the closed loop of this process.

Two different tomography sensors are used in this demonstration to measure the moisture: Electrical Capacitance Tomography (ECT) sensor and Microwave Tomography (MWT) sensor. Both sensors measure the 2D/3D electrical permittivity of the target which strongly correlates with the moisture content. The calculated moisture from ECT or MWT is then used as the input to the controller.

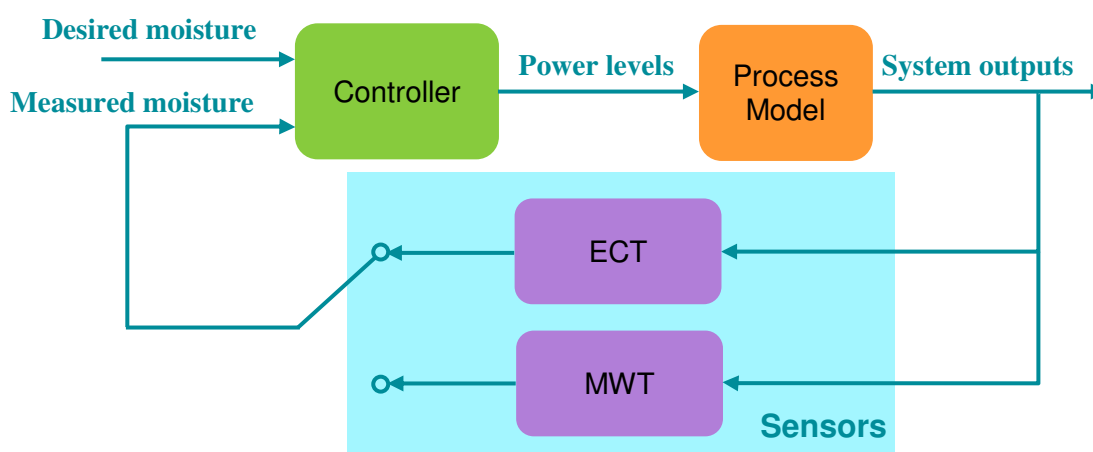


Figure 7: Microwave drying process closed loop

3.1. ECT

The ECT sensor consists of several electrodes mounted around the target. By applying electrical voltage to one of the electrodes, the electrical capacitances between the other electrodes can be measured. By repeating this measurement procedure by having each of the electrodes as a source, the electrical permittivity of the target can be reconstructed. Fig. 8 shows the designed and built ECT sensor for this demonstration using 12 electrodes on the top and bottom surfaces. MATLAB and NetGen software are used to design the sensor geometry and create its mesh.



TOMOCON				GRANT AGREEMENT No.: 764902		
Deliverable Title: Virtual Process Tomography Data for TOMOCON Demonstrations						
Del. Rel. No.	EU Del. No.	WP No.	Lead Beneficiary	Type	Date	
D2.2.	D6	WP2	UEF	Report	06.09.2019	

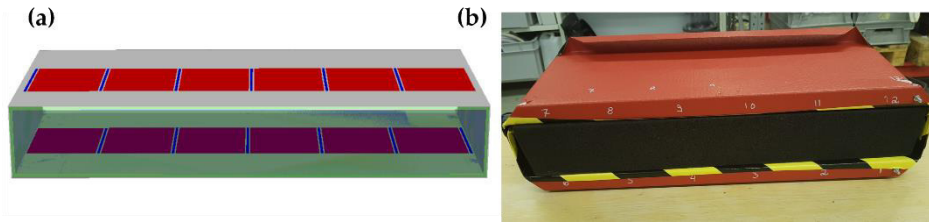


Figure 8: ECT sensor prototype (a) NetGen design (b) The built sensor while measuring the permittivity of an impregnated foam sample

In ECT, the forward and inverse problems are solved. In the forward problem, the inter-electrode capacitances are computed using the given permittivity distribution and excitation voltage. In the inverse problem, the internal permittivity is reconstructed based on the measured capacitances.

In virtual ECT, the real measurements of inter-electrode capacitances are not available. Therefore, the forward problem is employed to produce the simulated data needed for reconstruction using a given (true) permittivity distribution. In reality, this data is directly measured. Fig. 9 illustrates an example case of true permittivity distribution. After solving the forward and inverse problems, the electrical permittivity is reconstructed, which is shown in Fig. 10. As seen, the reconstructed image is very close to the true distribution. In the virtual demonstration and also in the real measurement case, the time resolution of the ECT system is around 25 Hz.

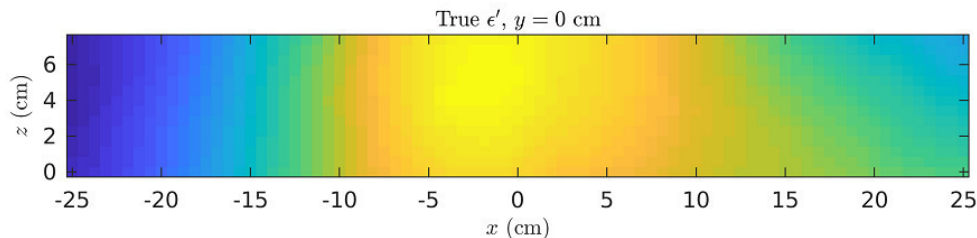


Figure 9: True permittivity distribution

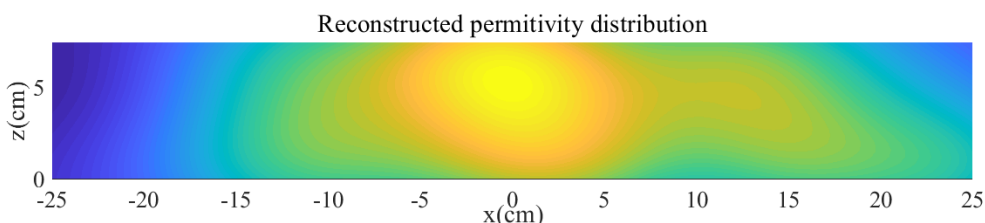


Figure 10: ECT permittivity reconstruction



TOMOCON				GRANT AGREEMENT No.: 764902	
Deliverable Title: Virtual Process Tomography Data for TOMOCON Demonstrations					
Del. Rel. No.	EU Del. No.	WP No.	Lead Beneficiary	Type	Date
D2.2.	D6	WP2	UEF	Report	06.09.2019

3.2. Microwave tomography

Microwave tomography (MWT) is used as an imaging modality to reconstruct the moisture content distribution in porous foam during its microwave drying process.

MWT is a technique of estimating the material properties (dielectric constant, conductivity) of an object from the measured data of a scattered electromagnetic field. An antenna array system is used to measure the scattered electric field in terms of S-parameter. The MWT setup for the present work is shown in Fig. 11.

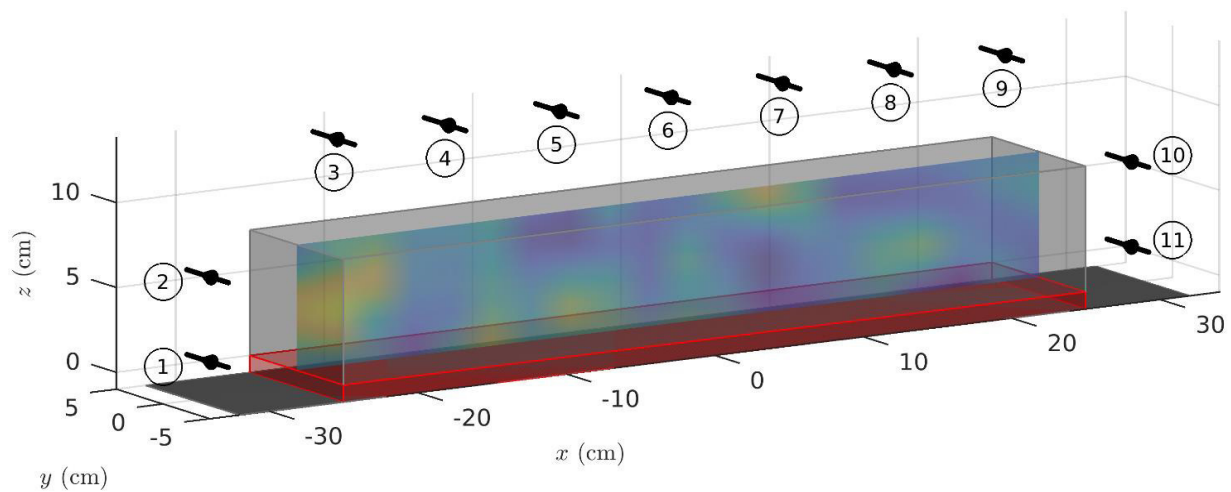


Figure 11: Model used for benchmarking purposes. The light gray box is the porous foam and the red box the conveyor belt while the dark gray surface denotes the perfect electric conductor (PEC) boundary. The antenna array is visualized with black cylinders and the color surface inside the porous foam illustrates the potential moisture density field on the cross section where $y=0$ cm.

In order to develop a microwave tomography (MWT) system, which is capable to extract the moisture distribution and moisture level inside the foam and distinguish between different moisture levels, the proper operation frequency should be obtained as the first step. Based on this operation frequency, a suitable Horn antenna will be employed (chosen due to the overcoming the high power interference) to transmitting/receiving signal into the medium.

To account for this operation frequency, we consider a one-dimensional (1D) model for the impregnated foam (dry foam with moisture), which is illuminated by a normal plane wave as depicted in Fig. 12.

TOMOCON			GRANT AGREEMENT No.: 764902		
Deliverable Title: Virtual Process Tomography Data for TOMOCON Demonstrations					
Del. Rel. No.	EU Del. No.	WP No.	Lead Beneficiary	Type	Date
D2.2.	D6	WP2	UEF	Report	06.09.2019

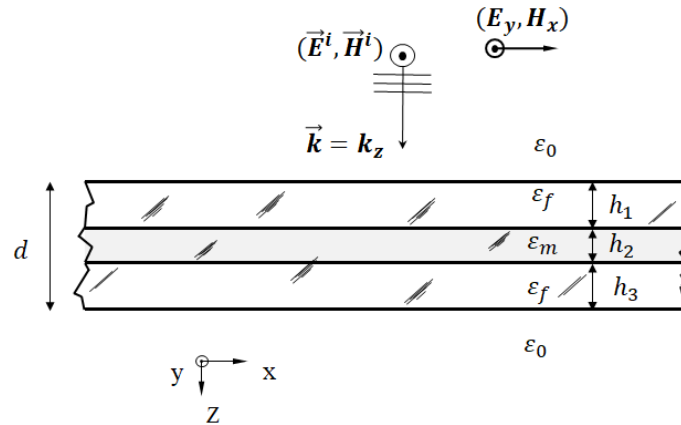


Figure 12: Cross section of a foam (with or without moisture) illuminated with a normal plane wave ($\theta=0$)

Permittivity used for simulating the above 1D model are summarized in Table 1. It should be mentioned that these parameters are obtained from measurements. The contents (M_n) are based on weight percentage and $M_n = \frac{W_w - W_d}{W_w} \times 100$ where W_w is the wet weight of the foam, W_d is the weight of the dry foam.

Table 1: Different moisture level parameters based on the measurements

Moisture Content (M_n %)	Real Part of Permittivity	Imaginary Part of Permittivity
Dry foam	1.164	0.0053
13	1.374	0.0587
15	1.414	0.0659
17	1.454	0.0731
25	1.613	0.102
50	2.318	0.1734

The amplitudes of the different return loss (RL or S_{11}), associated to the different moisture levels are shown in Fig. 13. Different frequency regions are separated using horizontal lines. As can be perceived from this figure, below C-band and in C-band, it is not possible to distinguish between different moisture levels. However, in X and Ku band it is easier to distinguish between different S-parameters. Upper band are not good options for this specific application due to the small penetration depth.

TOMOCON				GRANT AGREEMENT No.: 764902	
Deliverable Title: Virtual Process Tomography Data for TOMOCON Demonstrations					
Del. Rel. No.	EU Del. No.	WP No.	Lead Beneficiary	Type	Date
D2.2.	D6	WP2	UEF	Report	06.09.2019

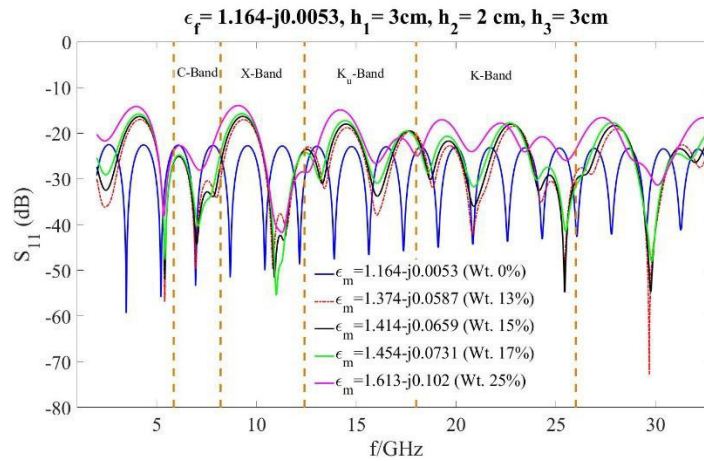


Figure 13: Return loss (S_{11}) of different moisture level

Associated to the operation frequency a Horn antenna will be designed for neural network (NN) to obtain moisture distribution and levels as the real MWT scenario is depicted in Fig. 14. Details of the NN method and results are given in the following.

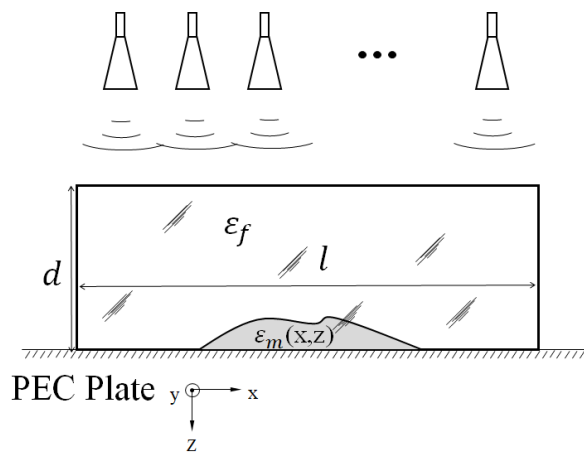
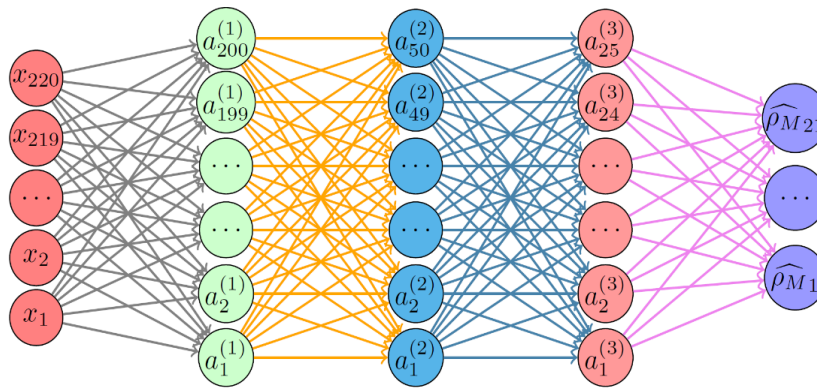


Figure 14: Cross section of real MWT scenario

The finite element method is chosen to simulate electromagnetic wave propagation (forward model) while a deep learning technique is used to estimate the moisture distribution of a porous foam from the measured scattered electric field data. In our present study, the neural network is trained with different moisture sample scenarios and their associated scattered electric field data from COMSOL simulation. The moisture samples, modelled as Gaussian random fields are based on the laboratory measurements (Karlsruhe Institute of Technology, Institute for Pulsed Power and Microwave Technology, Germany) by which the mathematical relation between moisture content and complex permittivity $\epsilon = \epsilon' - i\epsilon''$ is known with acceptable accuracy. This relation can be used to recover the physical parameters from the sampled moisture content distribution. One of the goals is to build a comprehensive database of different moisture content scenarios and the corresponding forward simulations that can further be used in machine learning based tools to recover the unknown moisture distribution from experimental data (in real time).

TOMOCON				GRANT AGREEMENT No.: 764902	
Deliverable Title: Virtual Process Tomography Data for TOMOCON Demonstrations					
Del. Rel. No.	EU Del. No.	WP No.	Lead Beneficiary	Type	Date
D2.2.	D6	WP2	UEF	Report	06.09.2019



Input layer Hidden layer1 Hidden layer2 Hidden layer3 Output layer

Figure 15: The multilayer deep fully connected network used in this study

The neural network architecture used in this work is shown in Fig. 15. It comprises three fully connected hidden layers while for the activation we choose the non-linear Rectified Linear Unit (ReLU).

For the training of the neural network, we generated a dataset comprising 15,000 moisture samples. The real and imaginary part of the complex-valued measurement data i.e. S-parameter is vectorized and given as an input to the neural network. Since we are interested to monitor a drying process of porous foam on a cross section on y-axis, an adequate resolution of the moisture density field of around 5cm x 2.5cm is chosen for the estimation. Moisture content estimate shown in Fig. 16 is an example from test data of low moisture content level.

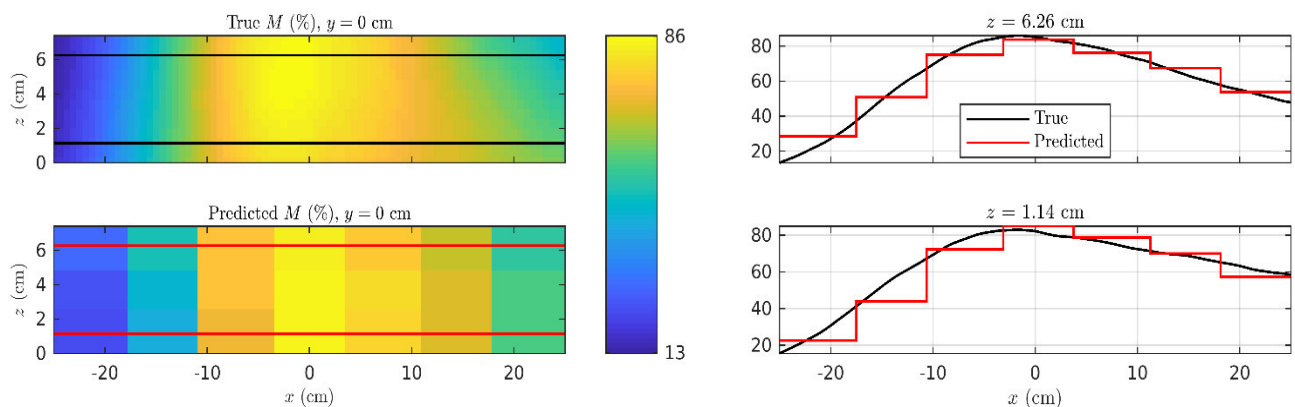


Figure 16: Pictures on the left show the true and predicted field values and pictures on the right for one row and column, respectively. The selected lines are visualized with black and red horizontal lines on the corresponding field graphs.



TOMOCON				GRANT AGREEMENT No.: 764902	
Deliverable Title: Virtual Process Tomography Data for TOMOCON Demonstrations					
Del. Rel. No.	EU Del. No.	WP No.	Lead Beneficiary	Type	Date
D2.2.	D6	WP2	UEF	Report	06.09.2019

3.3. Visual analytics and interactive visualisation for process tomography virtual demonstration

In our demonstrator, microwave drying for porous foams, there is an important part which is that the operators are supposed to better communicate and interact with the process to obtain more intuitive and straightforward insights, so that they are able to control and adjust the demonstrator more easily. For process condition monitoring, there are some infrared cameras mounted on the top surface of the chamber which are used to record the whole drying process. After capturing a large amount of infrared images frame by frame from infrared videos, we are eligible to do condition monitoring using deep learning via those images. The areas of high moisture, low moisture could be detected precisely as well as the fault area if existing.

In our case, each image captured will be labelled as a condition based on the types of moisture levels contained, e.g.: Fig. 17 has three types of moisture levels - high (red area), medium (green area) and low (blue area). We tend to train a large amount of images using deep learning and predict an unlabeled image with the output of a specific condition.

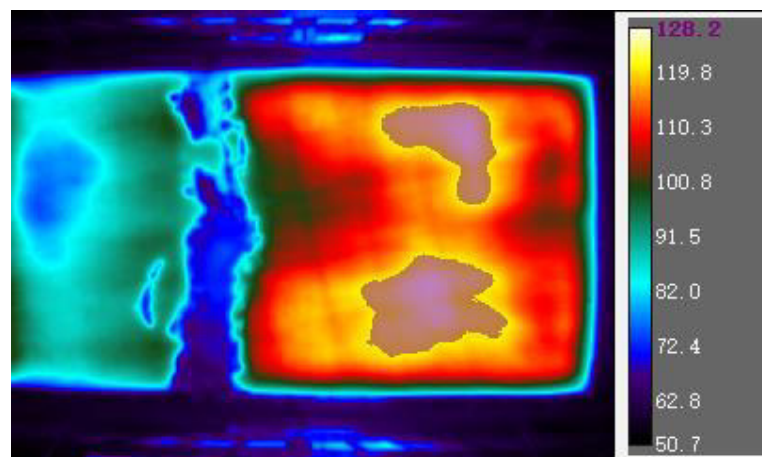


Figure 17: Example of infrared image

After the drying process, the MWT and ECT images will be reconstructed to detect the moisture distribution. The moisture distribution boundaries could be automatically detected and marked on the tomographic images, which can be regarded as a kind of visualisation. In our case, we proposed an automatic segmentation method--MWTS-KM--to visualize the low moisture area in MWT images (Fig. 18). Fig. 19 illustrates some examples of our samples experimented. This work is published in VINCI 2019. Furthermore, as long as we use more kinds of data, more interactive visualisation will be generated. For instance, changing different colour maps or colour modes to conduct visualization and then model the human perception will be the main research focus. Once we have different modalities of visualisations, it will be suitable to design a guideline for operators to understand and interact



TOMOCON			GRANT AGREEMENT No.: 764902		
Deliverable Title: Virtual Process Tomography Data for TOMOCON Demonstrations					
Del. Rel. No.	EU Del. No.	WP No.	Lead Beneficiary	Type	Date
D2.2.	D6	WP2	UEF	Report	06.09.2019

with different visualisations in our industrial tomography. This work will need onsite user studies or user interviews to collect human factors.

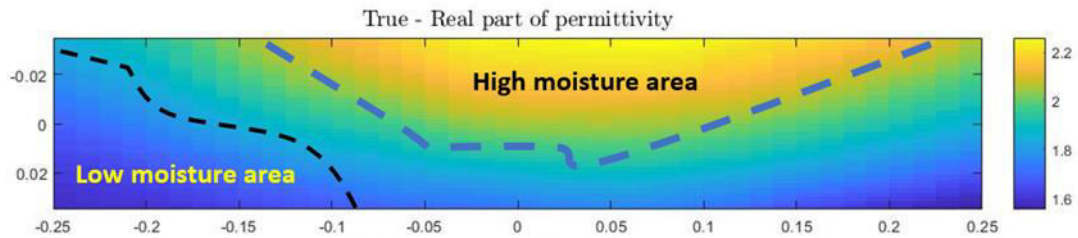


Figure 18: Example of MWT image

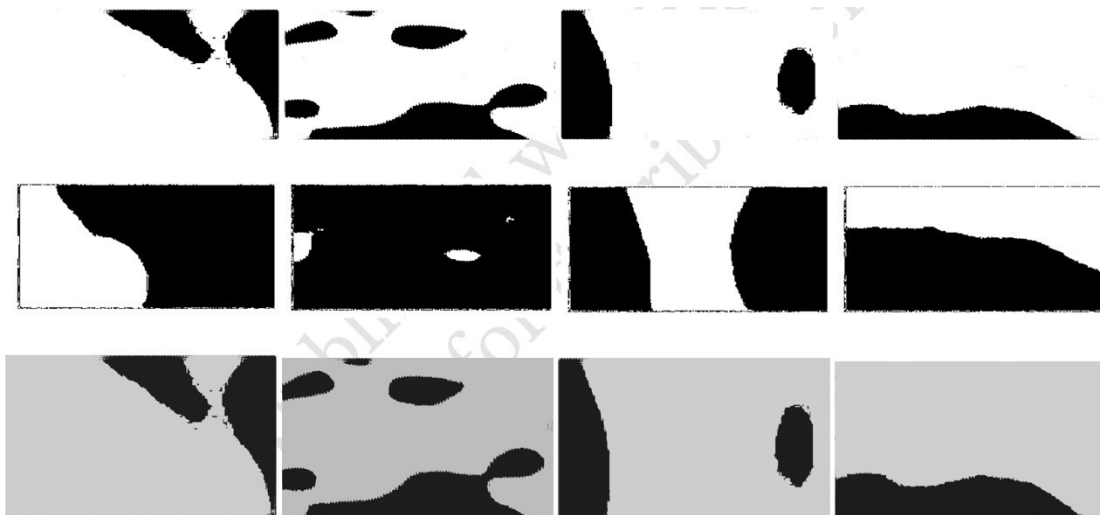


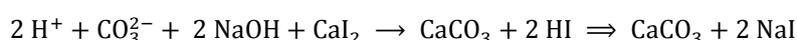
Figure 19: The comparison among three segmentation results. The first row stands for the results by using Otsu algorithm, the second row for results using conventional K-means algorithm and the third row for results using the proposed MWTS-KM algorithm.



TOMOCON				GRANT AGREEMENT No.: 764902	
Deliverable Title: Virtual Process Tomography Data for TOMOCON Demonstrations					
Del. Rel. No.	EU Del. No.	WP No.	Lead Beneficiary	Type	Date
D2.2.	D6	WP2	UEF	Report	06.09.2019

4. Tomographic sensors for virtual demonstration of semi-batch crystallization

It is proposed to use the reaction type crystallization for the semi-batch precipitation of calcium carbonate CaCO_3 . The feed solution is dissolved CO_2 at pH 12 using NaOH , and the receiving solution in the reactor is a CaI_2 -water solution. Due to the fast-chemical reaction, the precipitation process is greatly affected by mixing intensity (mesomixing), which can be controlled to obtain particles of desired size distribution. The following chemical equation is proposed,



The process flowsheet is shown in Figure 20.

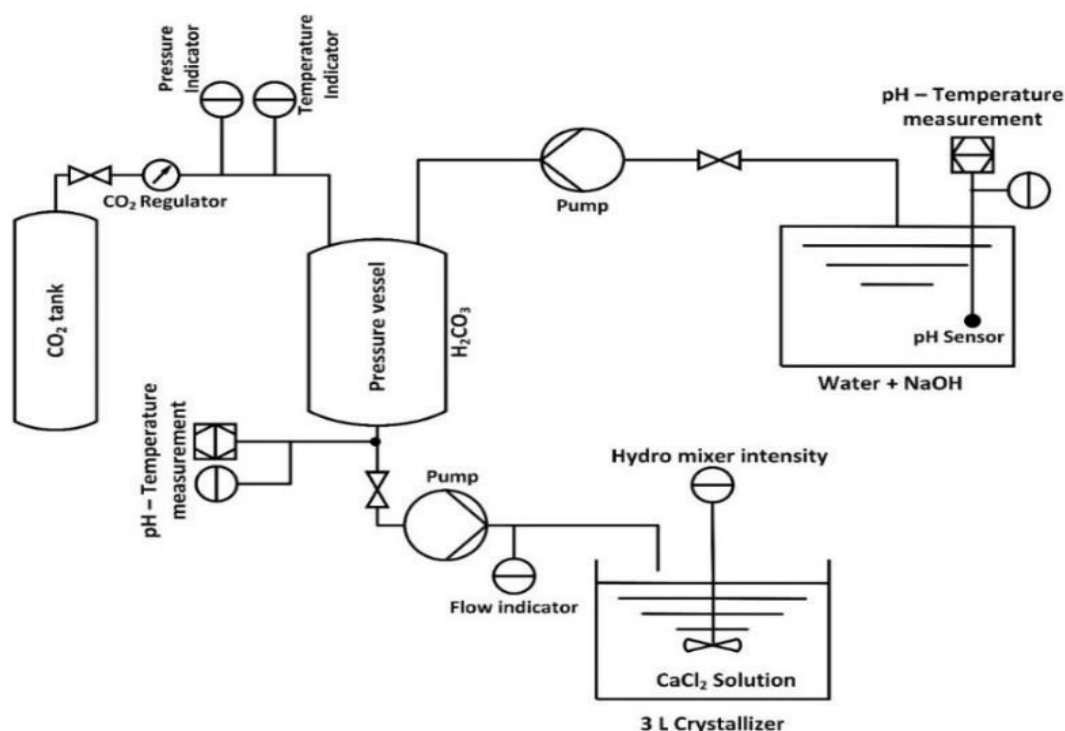


Figure 20: Semi-batch crystallization process of CaCO_3 using dissolved CO_2

4.1. Impedance tomography in semi-batch crystallization

It is expected from the Electrical Resistance Tomography (ERT) device to evaluate the differences in the solid density inside the reactor during the above-mentioned chemical reaction. The denser regions within the reactor would have a different conductivity as



TOMOCON			GRANT AGREEMENT No.: 764902		
Deliverable Title: Virtual Process Tomography Data for TOMOCON Demonstrations					
Del. Rel. No.	EU Del. No.	WP No.	Lead Beneficiary	Type	Date
D2.2.	D6	WP2	UEF	Report	06.09.2019

compared to the regions with lesser density. Along with this, the suspension height would be measured vertically. The solid suspension height is directly proportional to crystal size and crystal suspension density. The distribution can be measured using 3D-ERT inverse imaging methods in the horizontal plane, whereas vertical evaluations can be complemented to these measurements using 1-D point-to-point conductivity evaluations.

Physical meaning- The solid suspension height will be proportional to the crystal sizes. It would be measured using the horizontal and vertical conductivity differences in the reactor.

Uncertainties- Differentiating between dense CaI_2 converted into CaCO_3 . There is a possibility of low Signal-to-Noise Ratio (SNR) between the pixels of CaI_2 and CaCO_3 which would be a challenge.

Data formats- Images are in TIFF/JPEG format and 1D measurements are numerical. There is a possibility to include a phase-shift data if it provides useful information.

Protocols- Measurement would be observed at four points starting from the initial state to the end of the crystallization process as shown in Figure 21.

Sampling frequencies- The ERT system functions at a data sampling rate of 156k samples per second.

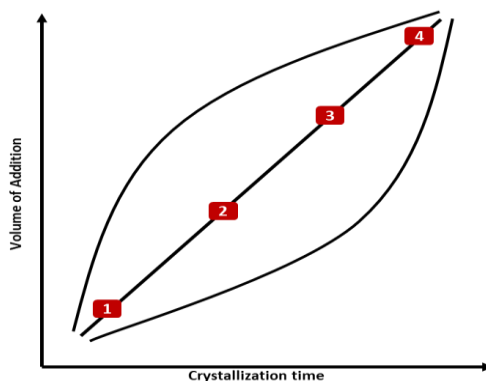


Figure 21: Tomographic measurement setpoints during the crystallization process

4.2. Ultrasound computed tomography for semi-batch crystallization

To design a controller for the above-mentioned semi-batch crystallization process, measurements related to crystal size distribution (CSD) are required. In these processes the solid-suspension density height is directly proportional to crystal size and crystal suspension. According to this, there is a great need of measuring the continuously changing density of the suspension. Ultrasound computed tomography (USCT) will aid towards this direction by utilizing a sound-speed imaging. An ultrasound travel-time inversion will be applied. By reconstructing the velocity distribution of the medium using tomographic data one could get meaningful information not only about the solid-suspension density height but also about the spatial distribution of densities. Related state-of-the-art research has shown a clear relation to sound-speed and density and adiabatic compressibility values.

Sound-speed imaging based on transmission ultrasound tomography method has been developed and tested with experimental work focused on slurry mixtures with different



TOMOCON			GRANT AGREEMENT No.: 764902		
Deliverable Title: Virtual Process Tomography Data for TOMOCON Demonstrations					
Del. Rel. No.	EU Del. No.	WP No.	Lead Beneficiary	Type	Date
D2.2.	D6	WP2	UEF	Report	06.09.2019

particle concentrations. Initial results of sound speed measurements at different concentrations are displayed in Figure 22. Furthermore, a 2D reflection ultrasound reconstruction software package has been developed to facilitate the reconstruction process.

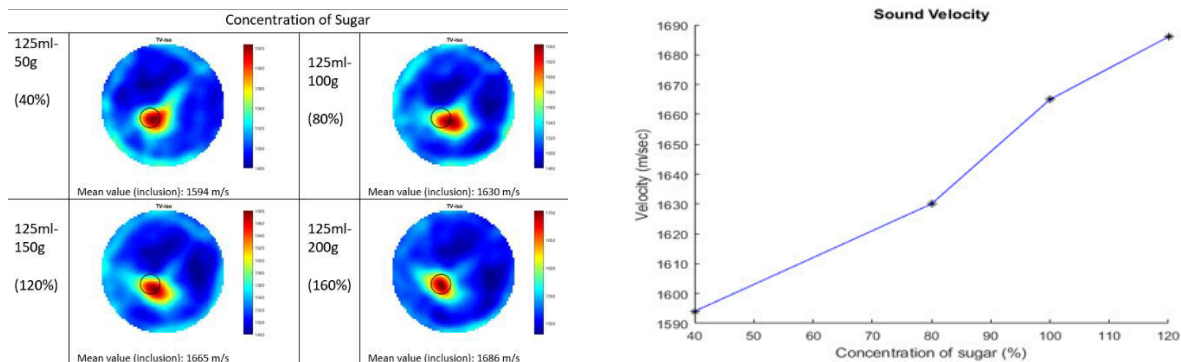


Figure 22: Ultrasound tomography measurements of different sucrose concentrations and 2D reflection reconstruction data

In the proposed semi-batch crystallization scenario of calcium carbonate, undersaturated solutions of CaI_2 -water is used; the feed solution is dissolved CO_2 at a predefined pH level. During the crystallization, the solution concentration drop will be around 10-50 g/L when CaCO_3 solid crystals are formed. After the nucleation point small crystals of micron size will start forming, which in turn will gradually change the concentration of crystals in the slurry. USCT will focus on characterizing the process by monitoring these density changes and detecting specific concentrations' levels. USCT will be focused on identifying four different density points of the constantly changing suspension (Figure 21). The imaging system will provide sound speed values as a correlated input to the controller. A key correlation will be made to relate the sound speed measurements to overall suspension density and total mass of crystals formed during the crystallization process.

4.3. Tomographic output data in PID controller design of a crystallization process

Measuring and controlling a single particle (10-15 microns) with current tomographic technologies is not feasible and practical. However, tomographic measurements (electrical resistance tomography or transmission ultrasound tomography) are able to visualize and quantify the final suspension height (H_s) and density. At various solution volume setpoints during a precipitation process, it is expected that the values of resistance (or transmission) vary due to chemical reaction and later on settlement of particles.

Since the hindered settling velocity of particles is a function of particle diameter, our objective is to correlate that parameter to feed flow rate and tomographic reconstructions in order to be used as an input for the PID controller. Figure 23 displays the closed loop of the crystallization system by coupling a virtual sensor output to a PID controller within the MATLAB/SIMULINK R2019a software. Eventually, the controller, by manipulating the key process variable (feed flow rate), evaluates a desired mean particle diameter.



TOMOCON				GRANT AGREEMENT No.: 764902	
Deliverable Title: Virtual Process Tomography Data for TOMOCON Demonstrations					
Del. Rel. No.	EU Del. No.	WP No.	Lead Beneficiary	Type	Date
D2.2.	D6	WP2	UEF	Report	06.09.2019

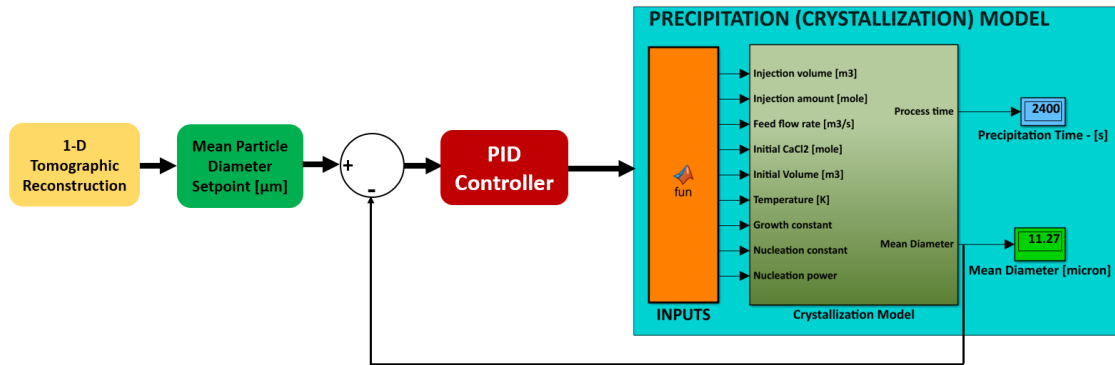


Figure 23: Final vision of the process model with PID controller in MATLAB/SIMULINK

